

Model	Deep Supervision	IN Top-1 (%)
<i>Supervised learning</i>		
Supervised Cls.		81.2
Supervised Cls.	✓	80.1 (-1.1)
Supervised Cls.‡	✓	80.6 (-0.6)
<i>Self-supervised pre-training</i>		
MAE		82.6
DeepMIM-MAE	✓	83.4 (+0.8)
DeepMIM†-MAE	✓	83.6 (+1.0)

Table 1: **Deep supervision benefits self-supervised pre-training.** We compare the effect of deep supervision during supervised learning and self-supervised pre-training, respectively, and report top-1 accuracy on ImageNet (IN). The experiment adopts a DeiT-style [43] training paradigm to optimize ViT-B on supervised image classification. We pre-train MAE and DeepMIM on MAE for 300 epochs on ViT-B. ‡: that hyper-parameters are carefully tuned. DeepMIM†: DeepMIM with hybrid targets (optional).

on image patches: the encoder (*i.e.*, ViT) generates the latent representations from the last Transformer block, while the decoder predicts the reconstruction targets of the masked patches. When transferring the MIM pre-trained model to downstream tasks, the encoder is retained while the decoder is dropped. As a result, the decoder implicitly deepens the network during the pre-training stage, making the shallower layers of the encoder receives weaker informative feedback from the supervision signal.

To drive the shallower layers learn more meaningful representations, we present DeepMIM, a ViT pre-training framework with deep supervision applied to MIM pretext task: we pre-train an MAE (on ViT-B) with three extra lightweight decoders appended to the outputs of the shallow blocks (the 6th, 8th and 10th blocks) of the encoder (ViT-B). Then ViT-B is finetuned on ImageNet-1K [9], following common practice [15]. Surprisingly, a substantial improvement (+0.8 top-1 accuracy) over the baseline (ViT-B pre-trained via the original MAE) is observed in Tab. 1, highlighting the potential benefits of deep supervision in MIM pre-training.

To investigate the benefits of introducing deep supervision into MIM pre-training, we comprehensively study several factors including 1) reconstruction loss of MAE and DeepMIM; 2) CKA (centered kernel alignment) [26] similarities between features produced by the intermediate layers and features produced by the last layer in DeepMIM; 3) attention diversities of different attention heads. In Fig. 3, we find that DeepMIM applied to MAE attains lower reconstruction losses across various layers in comparison with MAE. Xie *et al.* [55] also reveal that the lower the reconstruction loss

on the validation set is, the better performance of MIM is. In addition, we also observe that CKA scores between the last and shallow layers of DeepMIM always surpass those of MAE (Fig. 4) and DeepMIM learns more diverse attention heads than MAE (Fig. 6).

Recent MIM works have studied the question: *what* are appropriate reconstruction targets? Proposals have included discrete tokens [2], RGB pixels [15, 54], histograms of oriented gradients [48] and CLIP features [35, 23]. Our work dedicates to studying an orthogonal component of MIM pre-training: *where* should the reconstruction loss be applied? Therefore, our DeepMIM is compatible with a broad range of encode-decoder MIM models as shown in Fig. 1. Incorporating DeepMIM into various MIM models including MAE, and several other MAE variants with different reconstruction targets yield consistent improvements over the non-DeepMIM baselines. With parallel small decoders, DeepMIM only brings slightly more computation costs. The contributions of this work can be summarized as follows:

- We revisit the deep supervision for MIM pre-training. In contrast to previous MIM works exploring *what* form appropriate reconstruction targets should take, we focus on an orthogonal direction: *where* to apply the reconstruction loss. We thoroughly investigate the benefits of introducing deep supervision into MIM pre-training and find that it results in lower reconstruction loss, more diverse heads, and more powerful representation capability of the shallower layers.
- We present an optional module termed hybrid target generator, which further boosts the performance but involves extra computational overhead. A comparison with DeepMIM-MAE and MAE is shown in Tab. 1.
- DeepMIM is complementary to most existing MIM works. Extensive experiments demonstrate that MIM models equipped with DeepMIM significantly outperform their non-DeepMIM counterparts. For instance, using ViT-B, MAE with DeepMIM achieves 84.2 top-1 accuracy on ImageNet, outperforming MAE by +0.6 top-1 accuracy. By using DeepMIM with a strong reconstruction tokenizer, CLIP, we achieve state-of-the-art performance on various downstream tasks including image classification (85.6 top-1 accuracy on ImageNet-1K), object detection (52.8 AP^{box} on COCO) and semantic segmentation (53.1 mIoU on ADE20K).

2. Related Work

Self-supervised learning. Self-supervised pretraining aims to induce the model to learn transferable representations via a proxy task that does not require labels. One approach that has seen widespread adoption is to employ a contrastive loss, modeling the similarity between different views of

the same image and the dissimilarity between different images [49, 5, 16, 37, 53, 49, 47]. Recently, inspired by the success of BERT [10] in natural language processing with Masked Language Modeling, masking approaches (particularly Masked Image Modeling) have become a popular alternative for computer vision pretraining.

Masked image modeling. Masked Image Modeling operates by removing a portion of the input image before it is passed to the model and training the model to reconstruct the missing content. In the same spirit as masked language modeling, MAE [15] and SimMIM [54] employ raw pixels as the targets for reconstruction. In contrast to the tokens employed as reconstruction targets in natural language processing (which exhibit rich semantics), the pixels in computer vision convey a relatively low-level signal and typically exhibit considerable redundancy. To inject more semantics into target tokens, several proposals for the design of an appropriate tokenizer have been put forward. BeiT [2] and PeCo [11] employ VQVAE [38] to predict discrete visual vocabularies. MaskFeat [48] employ HOG (local gradient features) as a lightweight tokenizer with minimal parameters. iBOT [58] and data2vec [1] use the exponential moving average of the model as their tokenizer, inspired by contrastive learning approaches. Our method is compatible with previous methods and brings consistent improvements when used in combination with them.

Deep supervision. Deep Supervision [44, 27, 56, 29] was studied in the past as a tool to assist with training deep nets that could potentially mitigate gradient vanishing/exploding [22] problems. GoogleNet [40] introduces two extra supervision on intermediate layers. DSN [44] propose to design auxiliary supervision branches at certain intermediate layers. With the emergence of batch normalization [24] and residual learning [18], gradient vanishing/exploding issues appear to be less prevalent. It may be for this reason that deep supervision has received less interest recently. Differently from prior work, we revisit deep supervision in the context of self-supervised learning and masked image modeling and demonstrate its value in this setting.

3. Methodology

As shown in Fig. 2, DeepMIM adopts an encoder-multi-decoder architecture to perform the mask-and-predict task for ViT pretraining. For concreteness, we use MAE [15] to illustrate our underlying approach. Nevertheless, DeepMIM can be applied to various masked image modeling (MIM) frameworks—we describe how at the end of this section.

Encoder and multi-level features. We adopt ViT-B with 12 Transformer blocks as the encoder h_θ . Following ViT [12], we divide an input image x into regular non-overlapping patches. Then, similar to MAE [15], we randomly mask a high proportion of patches, yielding a masked image \tilde{x} . We then feed \tilde{x} into the encoder h_θ to produce multi-level

features.

Multi-decoder. Let g_ξ represent the default decoder attached to the last (12th) block. In addition to the last Transformer block, decoders are also attached to intermediate blocks. For ViT-B, we append three extra decoders (denoted g_ξ^1, g_ξ^2 and g_ξ^3) onto the 6th, 8th and 10th Transformer block of the encoder h_θ to facilitate deep supervision. Each decoder is an independent 4-layer Transformer with encoded visible patches (from the last block or intermediate blocks) and masked tokens as input. Thanks to the lightweight decoders, the overall training cost of DeepMIM is slightly higher than that of MAE, i.e., DeepMIM and MAE take 115 and 108 training hours respectively under a 1600-epoch schedule on $32 \times$ NVIDIA V100 GPUs. We use p and p_i to denote the reconstruction prediction by g_ξ and g_ξ^i , respectively.

Progressive hybrid targets (optional). The features produced by the shallower layers of the ViT are less discriminative. It may be beyond the capacity of these intermediate features to reconstruct the targets that are too complicated, i.e., raw pixels. As a by-product of MIM task, a pre-trained MAE is able to recover masked images. Though MAE produces fuzzy reconstruction results¹, we propose to use these reconstructed images as appropriate reconstruction targets to ease the learning of the intermediate blocks. We name a pre-trained MAE as a hybrid target generator, as illustrated in Figure 2. Concretely, given a masked image \tilde{x} , we feed it into a pre-trained MAE to generate a reconstructed image, denoted \hat{x} . The hybrid target t is generated by blending the raw image x and the reconstructed image \hat{x} with a blending ratio α :

$$t = \alpha x + (1 - \alpha)\hat{x}. \quad (1)$$

Let t_i represent the reconstruction target of the decoder g_ξ^i . We set α as 0, 1/3 and 2/3 for g_ξ^1, g_ξ^2 and g_ξ^3 , respectively.

Note that the hybrid targets are optional. Even though using hybrid targets improves fine-tuning performance, there is still additional computational overhead. We suggest to use hybrid targets only if there is an off-the-shelf hybrid target generator (a pre-trained MIM model). We use DeepMIM[†] to denote our framework with hybrid targets. For DeepMIM (without hybrid targets), we set $\alpha = 1$ for all decoders.

Training objective. The overall loss is the sum of the $M + 1$ ℓ_2 reconstruction losses produced by the M extra decoders and the primary decoder:

$$\mathcal{L} = \sum_{i=1}^M \|\mathcal{M}(t_i) - p_i\|_2^2 + \|\mathcal{M}(x) - p\|_2^2, \quad (2)$$

where $\mathcal{M}(\cdot)$ denotes the operation that extracts the targets of the masked patches, and M is the number of extra decoders. $M = 3$ for ViT-B.

¹Image inpainting is not the objective of MAE.

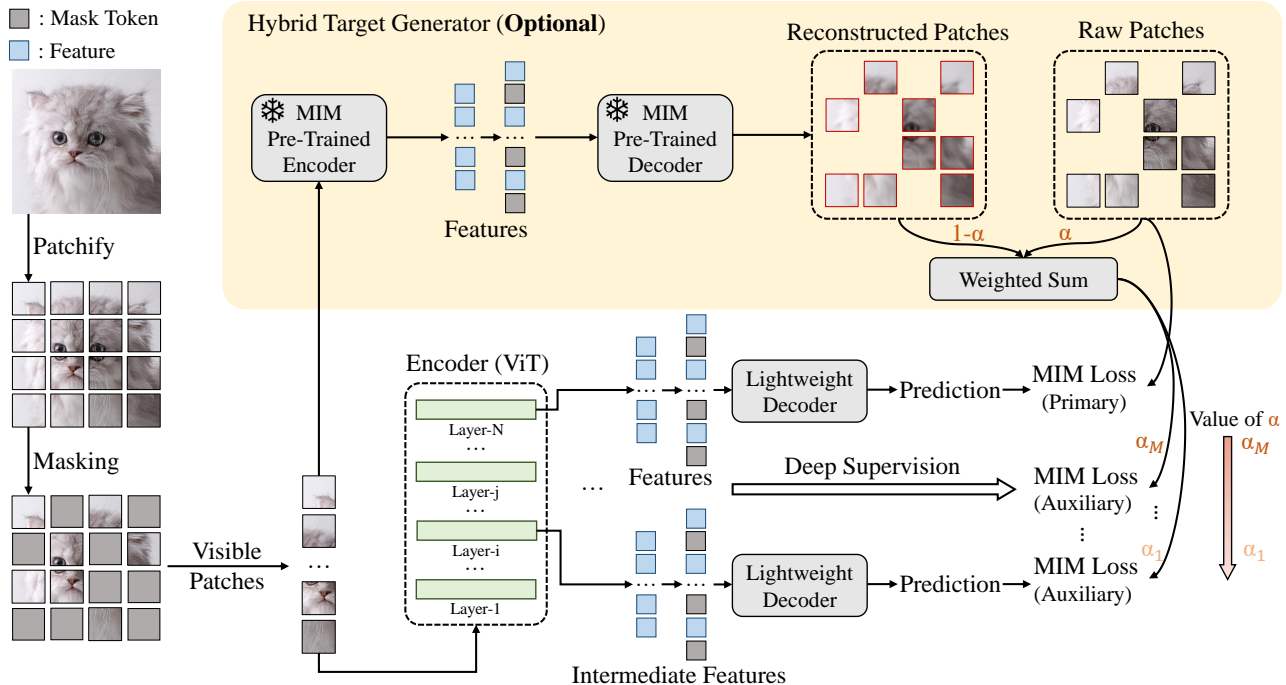


Figure 2: An overview of DeepMIM. DeepMIM applies deep supervision on intermediate features during pre-training. Each lightweight decoder is composed of 4 Transformer blocks. DeepMIM is compatible with many MIM models across a range of architectures and reconstruction targets. Using the hybrid target generator (a pre-trained MIM model) is an optional choice.

DeepMIM is compatible with a range of MIM models.

DeepMIM can be applied to a range of MIM models with different reconstruction targets, *e.g.*, RGB pixels [15, 54], discrete tokens [2], histograms of oriented gradients [48], CLIP features [23] and DINO features [4]. The implementation consists of four steps: 1) utilize an off-the-shelf MIM model to produce reconstructed signals for masked images (optional); 2) generate a collection of hybrid targets by integrating raw signals and reconstructed signals with a given blending ratio (optional); 3) append extra decoders to the intermediate Transformer blocks; 4) train the MIM model equipped with DeepMIM through the loss defined in Eq. 2.

4. Discussion

We compare MAE to MAE equipped with DeepMIM (DeepMIM-MAE) with respect to the loss, layer similarity and capability of shallower blocks. We adopt ViT-B for both methods. Both pre-training and fine-tuning are conducted on ImageNet-1K training set. Unless otherwise specified, we adopt a 300-epoch pre-training schedule.

Training and validation loss. In Fig. 3, we plot the training loss and the validation loss of MAE and DeepMIM-MAE on ImageNet-1K, respectively. For a fair comparison, we only show the reconstruction loss associated with the last block of the DeepMIM-MAE. We observe that DeepMIM-MAE

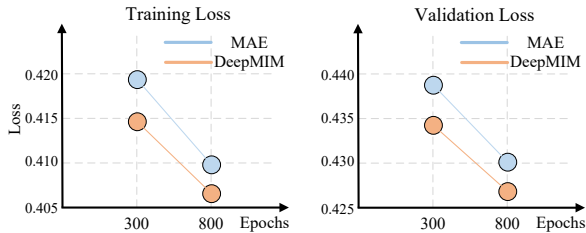


Figure 3: Comparison of the training loss (left) and the validation loss (right) of the MAE and our DeepMIM-MAE. We show only the reconstruction loss from the last block of the DeepMIM-MAE.

lowers the training loss across different training regimes (300 and 800 epochs). A recent work [55] shows that validation loss in pre-training is a good indicator for how well a model will perform during fine-tuning on downstream tasks. For completeness, we also report validation loss, showing the identical phenomenon—DeepMIM-MAE achieves a lower loss than MAE.

Feature similarity. We employ centered kernel alignment (CKA) [26] to identify correspondences between features produced by the last block and features produced by the intermediate blocks. The comparison between MAE and

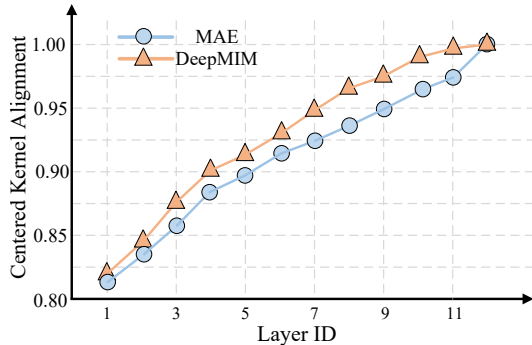


Figure 4: We use CKA [26] to evaluate the correspondences between the feature from the last block and the features from the intermediate blocks. Blue: MAE; red: DeepMIM-MAE.

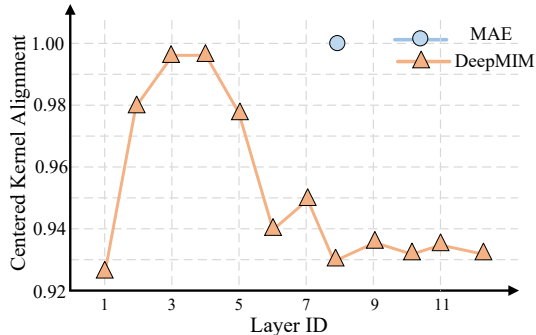
DeepMIM-MAE is shown in Fig. 4. From the first block to the penultimate block, the CKA score of DeepMIM-MAE always surpasses that of MAE, suggesting that the features from the intermediate blocks of DeepMIM-MAE are more discriminative.

Cross feature similarity. We use CKA to calculate similarities between features from the 8th block of MAE and features from all blocks of DeepMIM-MAE as shown in Fig. 5a. We also plot a reversed version in Fig. 5b. The MAE’s intermediate (8th block) features exhibit greatest alignment with DeepMIM-MAE’s shallower block features (3th and 4th). In contrast, the intermediate (8th block) features of DeepMIM-MAE align more closely with features from the deeper blocks (9th and 10th) of MAE. This study also indicates that DeepMIM significantly strengthens the discriminative power of the features from the shallower blocks.

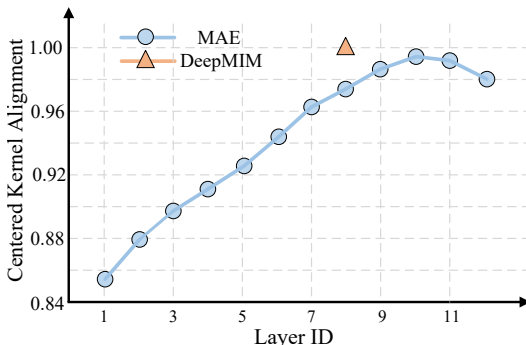
Attention Head Diversity. We calculate the cosine similarities between different attention heads to explore the head diversities. According to [52], more diverse heads indicate a stronger capacity for representation. As shown in Fig. 6, we plot the cosine similarities of different attention heads across various layers of MAE and DeepMIM. Our DeepMIM yields more diverse heads in comparison with MAE.

Fine-tuning the last-K blocks. To further assess the quality of the features from the shallower blocks, we freeze a subset of shallow blocks and fine-tune the remaining ones. For this experiment, we report top-1 accuracy on ImageNet. As shown in Fig. 7, when the number of trainable blocks is varied from 1 (only the last block is trainable) to 12 (all blocks are trainable), DeepMIM-MAE consistently outperforms MAE by a significant margin.

Randomly initialising the last-K blocks when fine-tuning. For this experiment, we first randomly initialize the last-K blocks of a pre-trained ViT-B, then the ViT-B is fine-tuned on ImageNet in an end-to-end manner. Fig. 8 shows a comparison between MAE and DeepMIM-MAE. We observe that DeepMIM-MAE consistently outperforms



(a) CKA similarity between the 8th layer of MAE and all layers of DeepMIM.



(b) CKA similarity between the 8th layer of DeepMIM and all layers of MAE.

Figure 5: Cross feature similarities evaluated by CKA.

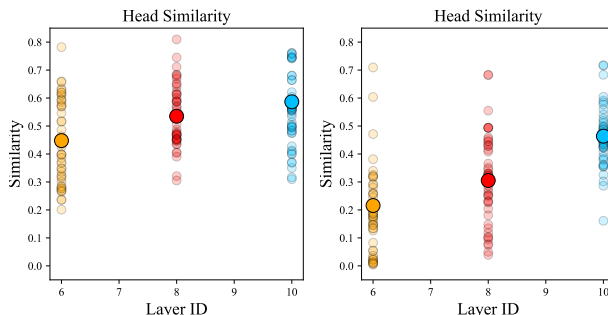


Figure 6: Comparison of the head cosine similarity of the MAE (left) and our DeepMIM-MAE (right) across different layers. Large dots denote the averaged similarities.

MAE in each case, demonstrating that good representations at shallow blocks are advantageous for the learning of deeper blocks particularly when they are randomly initialized.

5. Experiments

Implementation Details. We adopt ViT-B/16 as our backbone with input size of 224×224 . The ImageNet-1K image classification dataset is used for both pre-training and fine-tuning [9]. We apply our DeepMIM on MAE with RGB

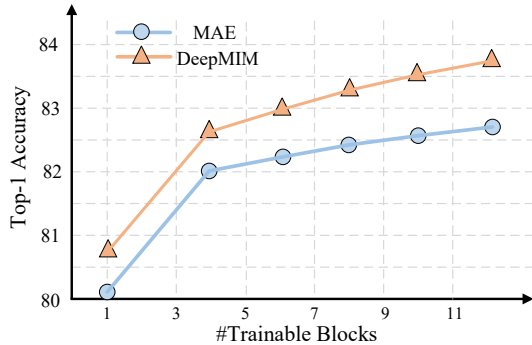


Figure 7: When varying the number of trainable blocks from 1 to 12, DeepMIM-MAE consistently outperforms MAE by apparent margins.

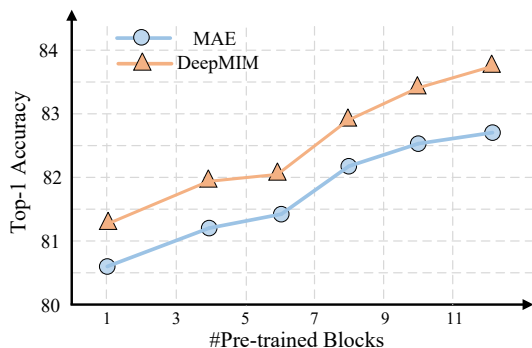


Figure 8: End-to-End finetune on ImageNet-1K. Start k layers are pretrained by MAE/Ours, and rest layers are randomly initialized.

pixels [15] and CLIP features [36]. For comparison with state-of-the-art methods, we pre-train DeepMIM for 300 and 1600 epochs. We follow the same training recipe of MAE [15], more details can be found in supplementary materials. We adopt the hybrid target generator (a pre-trained MIM model) if the reconstruction targets are pixels and detach it when using other reconstruction targets, since there are lots of off-the-shelf pre-trained MIM models with pixels as the reconstruction targets (e.g. from Huggingface). We use DeepMIM[†] to indicate DeepMIM with hybrid targets.

5.1. Main Results

Image Classification. In Tab. 2, we compare the fine-tuning results of various self-supervised pre-training methods on ImageNet-1K. We report the top-1 accuracy on the ImageNet validation set. Under a 300-epoch pre-training schedule, DeepMIM[†]-MAE (83.6) outperforms the MAE baseline (82.6) by +1.0. With a more powerful tokenizer like CLIP, DeepMIM-MAE-CLIP achieves 84.8 top-1 accuracy, outperforming the baseline of MAE-CLIP by +1.0.

When conducting a longer pre-training schedule (1600 epochs), DeepMIM[†]-MAE (84.2) surpasses MAE (83.6) by +0.6. DeepMIM-MAE-CLIP (85.6) outperforms MAE-CLIP

Method	Epochs	Target	Top-1
<i>ViT-B</i>			
BeiT [2]	300	DALL-E	83.2
CIM [13]	300	Pixel	83.3
CAE [6]	300	Momentum	83.6
MaskFeat [48]	300	HOG	83.6
iBoT [58]	400	Momentum	83.8
PeCo [11]	300	Codebook	84.1
MAE [15]	300	Pixel	82.6
DeepMIM-MAE	300	Pixel	83.4
DeepMIM [†] -MAE	300	Pixel	83.6
MAE-CLIP* [15]	300	CLIP	83.8
DeepMIM-MAE-CLIP	300	CLIP	84.8
<i>ViT-B + longer pre-training</i>			
DINO [4]	1600	Momentum	82.8
BEiT [2]	800	DALL-E	83.2
SimMIM [54]	800	Pixel	83.8
SIM [41]	1600	Momentum	83.8
CAE [6]	1600	Momentum	83.9
MaskFeat [48]	1600	HOG	84.0
iBoT [58]	1600	Momentum	84.0
PeCo [11]	800	Codebook	84.5
MAE [15]	1600	Pixel	83.6
DeepMIM-MAE	1600	Pixel	84.0
DeepMIM [†] -MAE	1600	Pixel	84.2
MAE-CLIP*	1600	CLIP	84.8
DeepMIM-MAE-CLIP	1600	CLIP	85.6

Table 2: Comparison with previous self-supervised pre-training methods on ViT-B/16. We report top-1 accuracy on ImageNet-1K. *: reproduced result. MAE-CLIP: an MAE variant with CLIP features as targets.

(84.8) by +0.8, achieving a new state-of-the-art.

Object Detection. Following common practice, we use the COCO [30] benchmark to evaluate the transferability of DeepMIM to the object detection task. We employ DeepMIM pre-trained ViT-B/16 as the backbone and Mask R-CNN [17] as the detector. We report AP^{box} AP^{mask} in Tab. 3. DeepMIM[†]-MAE outperforms the MAE baseline by +1.3 AP^{box} and +0.3 AP^{mask} . DeepMIM with MAE-CLIP achieves state-of-the-art performance of 52.8 AP^{box} and 46.0 AP^{mask} .

Semantic Segmentation. We also transfer the DeepMIM pre-trained ViT-B/16 to semantic segmentation on the ADE20K [57] benchmark. We use UperNet [50] for a fair comparison with previous methods. We report mean intersection over union (mIoU) for each model in Tab. 4. DeepMIM[†]-MAE outperforms its counterpart by +1.4, and DeepMIM-MAE-CLIP achieves the state-of-the-art performance of 53.1 mIoU.

Video Classification. This transfer experiment is conducted on Kinetics-400 [25] benchmark using ViT-B. We apply

Method	Epochs	AP ^{box}	AP ^{mask}
PeCo [11]	800	44.9	40.4
MoCo-v3 [7]	300	47.9	42.7
BEiT [2]	800	49.8	44.4
SIM [41]	1600	49.1	43.8
iBOT [58]	1600	51.2	44.2
CAE [6]	1600	50.1	44.0
MAE [15]	1600	50.3	44.9
DeepMIM [†] -MAE	1600	51.6	45.2
DeepMIM-MAE-CLIP	1600	52.8	46.0

Table 3: COCO [30] object detection and instance segmentation using Mask R-CNN [17].

Method	Epochs	mIoU
CIM [13]	300	43.5
BEiT [2]	800	47.1
MoCo-v3 [7]	300	47.3
DINO [4]	400	47.2
PeCo [11]	800	48.5
iBOT [58]	1600	50.0
CAE [6]	1600	50.2
MAE [15]	1600	48.1
DeepMIM [†] -MAE	1600	49.5
DeepMIM-MAE-CLIP	1600	53.1

Table 4: ADE20K [57] semantic segmentation using UperNet [50]

DeepMIM to VideoMAE [42], and report top-1 accuracy on Kinetics-400 validation set. We follow the same pre-training and fine-tuning settings of VideoMAE and pre-train DeepMIM-VideoMAE for 800 epochs for a fair comparison with VideoMAE. The results are reported in Tab. 5. DeepMIM-VideoMAE improves over the baseline VideoMAE by +1.2.

Robustness Evaluation on Out-of-domain Datasets. We evaluate DeepMIM-MAE on three out-of-domain datasets [21, 19, 20]: ImageNet-A (natural adversarial examples), ImageNet-R (semantic shifts), and ImageNet-C (image corruptions). We report top-1 accuracy on ImageNet-A/R and mCE error on ImageNet-C. The results are shown in Tab. 6, our DeepMIM significantly outperforms MAE baseline by large margins.

5.2. Analysis and Ablation Study

For all ablation studies, we adopt DeepMIM-MAE with a 300-epoch pre-training schedule and a 100-epoch fine-tuning schedule on ImageNet-1K (reporting top-1 accuracy). We employ ViT-B as the backbone.

The effectiveness of deep supervision and progressive hybrid

Method	Pre-Data	Top-1 Acc.
NL I3D [46]	ImageNet-1K	77.3
TANet [32]		79.3
TDN _{En} [45]		79.4
Video Swin [31]		80.6
TimeSformer [3]	ImageNet-21K	78.3
Motionformer [34]		80.2
VideoMAE [42]	Kinetics-400	80.0
DeepMIM-VideoMAE		81.2

Table 5: Kinetics-400 [25] video classification.

Method	IN-A [↑]	IN-R [↑]	IN-C [↓]
DeiT [43]	25.8	45.4	36.8
MAE [15]	33.6	50.0	37.8
DeepMIM-MAE-CLIP	52.0	64.5	33.0

Table 6: Robustness evaluation on out-of-domain datasets.

Deep Supervision	Hybrid Target	Top-1 Acc.
		82.6
✓		83.4
✓	✓	83.6

Table 7: Ablation study on the effectiveness of deep supervision and hybrid targets.

brid targets. DeepMIM presents two techniques: 1) appending extra decoders to the intermediate blocks of the encoder to enable deep supervision for MIM pre-training; 2) utilizing progressive hybrid targets as the reconstruction targets for intermediate features. Tab. 7 demonstrates the effectiveness of each proposed technique.

Deep Supervision. DeepMIM appends extra decoders onto the intermediate blocks of the encoder. Here we explore: 1) where to apply deep supervision; 2) how many blocks should be involved. We do not use progressive hybrid targets in this study for efficiency. The results are shown in Tab. 8. We compare several variants with MAE baseline, which uses a single decoder on the output of the last Transformer block. We conclude that: 1) Regardless of how many blocks are used for deep supervision, all variations outperform the baseline. 2) Deep supervision should be applied to the appropriate blocks. For instance, the variant with {3rd, 6th, 9th, 12th} blocks involved deep supervision performs worse than that involving {6th, 9th, 12th} blocks. 3) The configuration which involves {6th, 8th, 10th, 12th} blocks yields the best result, outperforming the MAE baseline by +0.8.

Progressive hybrid targets. In Sec. 3, we propose to generate hybrid targets for different intermediate blocks by blending raw signals and the reconstructed signals with a blending ratio of α that controls the ratio between them (see Eq. (1)). Here we study using different blending ratios for the config-

Intermediate Block	Last Block (12 th)	Top-1 Acc.
-	✓	82.6
6 th	✓	82.8
8 th	✓	82.9
9 th	✓	82.9
6 th , 9 th	✓	83.1
8 th , 10 th	✓	83.1
3 th , 6 th , 9 th	✓	83.0
4 th , 6 th , 8 th	✓	83.2
6 th , 8 th , 10 th	✓	83.4

Table 8: Study of deep supervision using DeepMIM-MAE. First row is an MAE baseline.

Config ID	Blending Ratio (α)				Top-1 Acc.
	6 th	8 th	10 th	12 th	
1	1	1	1	1	83.5
2	0	0	0	1	83.4
3	1/2	1/2	1/2	1/2	83.4
4	0	1/3	2/3	1	83.6

Table 9: Study of progressive hybrid targets. We vary the blending ratio α of the {6th, 8th, 10th, 12th} blocks.

Block	Decoder	Top-1 Acc.
6 th , 12 th	Shared	82.1
6 th , 12 th	Independent	82.9
6 th , 8 th , 10 th , 12 th	Shared	81.4
6 th , 8 th , 10 th , 12 th	Independent	83.4

Table 10: Comparison of shared or Independent decoder in deep supervision. All supervision is the raw patches except without hybrid targets.

uration that involves deep supervision on the {4th, 8th, 10th, 12th} blocks in Tab. 9. We observe a slight improvement for the configuration where the targets of the {4th, 8th, 10th} blocks are pure reconstructed signals. Adopting progressive hybrid targets ($\alpha = 0, 1/3, 2/3, 1$ for the 6th, 8th, 10th and 12th blocks) yields the best performance, achieving 83.6% top-1 accuracy.

Shared decoder or independent decoder. By default, DeepMIM appends independent decoders at intermediate blocks. We now examine the possibility of employing a single shared decoder for different blocks as shown in Tab. 10. Using a shared decoder significantly degrades the performance, possibly because the feature distributions of different blocks vary significantly from one to another.

DeepMIM with different reconstruction targets. Differently from reconstruction targets in natural language processing with rich semantics, reconstruction targets in computer vision are low-level pixels [15, 54]. Recent

Method	Target	Top-1 Acc.
MAE	Pixel	82.6
DeepMIM	Pixel	83.4 (+0.8)
MAE	HOG [48]	83.4
DeepMIM	HOG [48]	83.9 (+0.5)
MAE	DINO Features [4]	83.8
DeepMIM	DINO Features [4]	84.4 (+0.6)
MAE	Perceptual Codebook [11]	83.7
DeepMIM	Perceptual Codebook [11]	84.3 (+0.6)
MAE	CLIP Features [36]	83.8
DeepMIM	CLIP Features [36]	84.8 (+1.0)

Table 11: Comparison of our method with MAE models with different reconstruction targets. All models are pre-trained for 300 epochs. Our methods bring consistent improvements.

works [39, 15, 11] have explored more semantic reconstruction targets, *e.g.*, CLIP features [36]. We apply DeepMIM to different MAE variants whose targets are RGB pixels [15], HOG [48], DINO features [4], discrete tokens generated by perceptual codebook [11] and CLIP features [36]. As shown in Tab. 11, without bells and whistles, DeepMIM consistently outperforms its counterpart in each comparison. **Training Complexity.** Compared with MAE (on ViT-B), DeepMIM adopts four lightweight decoders and DeepMIM[†] extra utilizes a hybrid target generator (a pre-trained MIM model). In contrast to the original MAE decoder, which uses eight Transformer blocks, each lightweight decoder in our DeepMIM is made up of four blocks. Besides, we suggest to use the hybrid target generator only if a pre-trained MIM model is available. Therefore, The extra cost of DeepMIM[†] over DeepMIM is the inference of generating hybrid targets. The pre-training cost of DeepMIM and DeepMIM[†] are 115 hours and 119 hours respectively, which are slightly higher than 108 hours of MAE under a 1600-epoch pre-training schedule on 32×NVIDIA V100 GPUs.

6. Conclusion

In this paper, we shift our focus from designing reconstruction targets to the question of where to apply the reconstruction loss. We find intermediate features from shallower Transformer blocks also have predictive power for reconstruction and that improving these features during training improves the quality of learned representation over the whole model. Therefore, we propose DeepMIM that applies deep supervision on the intermediate features with extra decoders and hybrid targets to provide appropriate supervision for less discriminative intermediate features. Our experiments demonstrate that DeepMIM is compatible with a range masked image modeling frameworks and produces consistent improvements over strong baselines.

References

- [1] Alexei Baeovski, Wei-Ning Hsu, Qiantong Xu, Arun Babu, Jiatao Gu, and Michael Auli. Data2vec: A general framework for self-supervised learning in speech, vision and language. *arXiv preprint arXiv:2202.03555*, 2022. 3
- [2] Hangbo Bao, Li Dong, and Furu Wei. Beit: Bert pre-training of image transformers. *arXiv preprint arXiv:2106.08254*, 2021. 1, 2, 3, 4, 6, 7
- [3] Gedas Bertasius, Heng Wang, and Lorenzo Torresani. Is space-time attention all you need for video understanding? In *ICML*, 2021. 7
- [4] Mathilde Caron, Hugo Touvron, Ishan Misra, Hervé Jégou, Julien Mairal, Piotr Bojanowski, and Armand Joulin. Emerging properties in self-supervised vision transformers. In *ICCV*, pages 9650–9660. IEEE, 2021. 4, 6, 7, 8, 11
- [5] Ting Chen, Simon Kornblith, Mohammad Norouzi, and Geoffrey Hinton. A simple framework for contrastive learning of visual representations. In *ICML*, pages 1597–1607. PMLR, 2020. 3
- [6] Xiaokang Chen, Mingyu Ding, Xiaodi Wang, Ying Xin, Shentong Mo, Yunhao Wang, Shumin Han, Ping Luo, Gang Zeng, and Jingdong Wang. Context autoencoder for self-supervised representation learning. *arXiv preprint arXiv:2202.03026*, 2022. 6, 7
- [7] Xinlei Chen*, Saining Xie*, and Kaiming He. An empirical study of training self-supervised vision transformers. *arXiv preprint arXiv:2104.02057*, 2021. 7
- [8] Navneet Dalal and Bill Triggs. Histograms of oriented gradients for human detection. In *CVPR*, volume 1, pages 886–893. IEEE, 2005. 11
- [9] Jia Deng, Wei Dong, Richard Socher, Li-Jia Li, Kai Li, and Li Fei-Fei. Imagenet: A large-scale hierarchical image database. In *CVPR*, pages 248–255. IEEE, 2009. 2, 5, 11
- [10] Jacob Devlin, Ming-Wei Chang, Kenton Lee, and Kristina Toutanova. Bert: Pre-training of deep bidirectional transformers for language understanding. *arXiv preprint arXiv:1810.04805*, 2018. 3
- [11] Xiaoyi Dong, Jianmin Bao, Ting Zhang, Dongdong Chen, Weiming Zhang, Lu Yuan, Dong Chen, Fang Wen, and Nenghai Yu. Peco: Perceptual codebook for bert pre-training of vision transformers. *arXiv preprint arXiv:2111.12710*, 2021. 1, 3, 6, 7, 8, 11
- [12] Alexey Dosovitskiy, Lucas Beyer, Alexander Kolesnikov, Dirk Weissenborn, Xiaohua Zhai, Thomas Unterthiner, Mostafa Dehghani, Matthias Minderer, Georg Heigold, Sylvain Gelly, et al. An image is worth 16x16 words: Transformers for image recognition at scale. *arXiv preprint arXiv:2010.11929*, 2020. 1, 3
- [13] Yuxin Fang, Li Dong, Hangbo Bao, Xinggang Wang, and Furu Wei. Corrupted image modeling for self-supervised visual pre-training. *arXiv preprint arXiv:2202.03382*, 2022. 6, 7
- [14] Christoph Feichtenhofer, Haoqi Fan, Jitendra Malik, and Kaiming He. Slowfast networks for video recognition. In *Proceedings of the IEEE/CVF international conference on computer vision*, pages 6202–6211, 2019. 11
- [15] Kaiming He, Xinlei Chen, Saining Xie, Yanghao Li, Piotr Dollár, and Ross Girshick. Masked autoencoders are scalable vision learners. In *CVPR*, pages 16000–16009. IEEE, 2022. 1, 2, 3, 4, 6, 7, 8, 11
- [16] Kaiming He, Haoqi Fan, Yuxin Wu, Saining Xie, and Ross Girshick. Momentum contrast for unsupervised visual representation learning. In *CVPR*, pages 9729–9738. IEEE, 2020. 3
- [17] Kaiming He, Georgia Gkioxari, Piotr Dollár, and Ross Girshick. Mask r-cnn. In *ICCV*, pages 2961–2969. IEEE, 2017. 6, 7, 11
- [18] Kaiming He, Xiangyu Zhang, Shaoqing Ren, and Jian Sun. Deep residual learning for image recognition. In *Proceedings of the IEEE conference on computer vision and pattern recognition*, pages 770–778, 2016. 1, 3
- [19] Dan Hendrycks, Steven Basart, Norman Mu, Saurav Kadavath, Frank Wang, Evan Dorundo, Rahul Desai, Tyler Zhu, Samyak Parajuli, Mike Guo, Dawn Song, Jacob Steinhardt, and Justin Gilmer. The many faces of robustness: A critical analysis of out-of-distribution generalization. *ICCV*, 2021. 7
- [20] Dan Hendrycks and Thomas Dietterich. Benchmarking neural network robustness to common corruptions and perturbations. *ICLR*, 2019. 7
- [21] Dan Hendrycks, Kevin Zhao, Steven Basart, Jacob Steinhardt, and Dawn Song. Natural adversarial examples. *CVPR*, 2021. 7
- [22] Sepp Hochreiter, Yoshua Bengio, Paolo Frasconi, Jürgen Schmidhuber, et al. Gradient flow in recurrent nets: the difficulty of learning long-term dependencies, 2001. 3
- [23] Zejiang Hou, Fei Sun, Yen-Kuang Chen, Yuan Xie, and Sun-Yuan Kung. Milan: Masked image pretraining on language assisted representation. *arXiv preprint arXiv:2208.06049*, 2022. 2, 4, 11
- [24] Sergey Ioffe and Christian Szegedy. Batch normalization: Accelerating deep network training by reducing internal covariate shift. In *International conference on machine learning*, pages 448–456. PMLR, 2015. 1, 3
- [25] Will Kay, Joao Carreira, Karen Simonyan, Brian Zhang, Chloe Hillier, Sudheendra Vijayanarasimhan, Fabio Viola, Tim Green, Trevor Back, Paul Natsev, et al. The kinetics human action video dataset. *arXiv preprint arXiv:1705.06950*, 2017. 6, 7
- [26] Simon Kornblith, Mohammad Norouzi, Honglak Lee, and Geoffrey Hinton. Similarity of neural network representations revisited. In *International Conference on Machine Learning*, pages 3519–3529. PMLR, 2019. 2, 4, 5
- [27] Chen-Yu Lee, Saining Xie, Patrick Gallagher, Zhengyou Zhang, and Zhuowen Tu. Deeply-supervised nets. In *Artificial intelligence and statistics*, pages 562–570. PMLR, 2015. 1, 3
- [28] Gang Li, Heliang Zheng, Daqing Liu, Chaoyue Wang, Bing Su, and Changwen Zheng. Semmae: Semantic-guided masking for learning masked autoencoders. *arXiv preprint arXiv:2206.10207*, 2022. 11
- [29] Renjie Li, Xinyi Wang, Guan Huang, Wenli Yang, Kaining Zhang, Xiaotong Gu, Son N Tran, Saurabh Garg, Jane Alty, and Quan Bai. A comprehensive review on deep supervision:

- Theories and applications. *arXiv preprint arXiv:2207.02376*, 2022. 3
- [30] Tsung-Yi Lin, Michael Maire, Serge Belongie, James Hays, Pietro Perona, Deva Ramanan, Piotr Dollár, and C Lawrence Zitnick. Microsoft coco: Common objects in context. In *ECCV*, pages 740–755. Springer, 2014. 6, 7, 11
- [31] Ze Liu, Jia Ning, Yue Cao, Yixuan Wei, Zheng Zhang, Stephen Lin, and Han Hu. Video swin transformer. In *CVPR*, 2022. 7
- [32] Zhaoyang Liu, Limin Wang, Wayne Wu, Chen Qian, and Tong Lu. Tam: Temporal adaptive module for video recognition. In *ICCV*, 2021. 7
- [33] Ilya Loshchilov and Frank Hutter. Decoupled weight decay regularization. In *International Conference on Learning Representations*, 2018. 11
- [34] Mandela Patrick, Dylan Campbell, Yuki Asano, Ishan Misra, Florian Metze, Christoph Feichtenhofer, Andrea Vedaldi, and Joao F. Henriques. Keeping your eye on the ball: Trajectory attention in video transformers. In *NeurIPS*, 2021. 7
- [35] Zhiliang Peng, Li Dong, Hangbo Bao, Qixiang Ye, and Furu Wei. Beit v2: Masked image modeling with vector-quantized visual tokenizers. *arXiv preprint arXiv:2208.06366*, 2022. 2
- [36] Alec Radford, Jong Wook Kim, Chris Hallacy, Aditya Ramesh, Gabriel Goh, Sandhini Agarwal, Girish Sastry, Amanda Askell, Pamela Mishkin, Jack Clark, et al. Learning transferable visual models from natural language supervision. In *International Conference on Machine Learning*, pages 8748–8763. PMLR, 2021. 6, 8
- [37] Alec Radford, Jong Wook Kim, Chris Hallacy, A. Ramesh, Gabriel Goh, Sandhini Agarwal, Girish Sastry, Amanda Askell, Pamela Mishkin, Jack Clark, Gretchen Krueger, and Ilya Sutskever. Learning transferable visual models from natural language supervision. In *ICML*, 2021. 3
- [38] Aditya Ramesh, Mikhail Pavlov, Gabriel Goh, Scott Gray, Chelsea Voss, Alec Radford, Mark Chen, and Ilya Sutskever. Zero-shot text-to-image generation. In *ICML*, pages 8821–8831. PMLR, 2021. 3
- [39] Sucheng Ren, Fangyun Wei, Zheng Zhang, and Han Hu. Tinymim: An empirical study of distilling mim pre-trained models. 2023. 8
- [40] Christian Szegedy, Wei Liu, Yangqing Jia, Pierre Sermanet, Scott Reed, Dragomir Anguelov, Dumitru Erhan, Vincent Vanhoucke, and Andrew Rabinovich. Going deeper with convolutions. In *Proceedings of the IEEE conference on computer vision and pattern recognition*, pages 1–9, 2015. 1, 3
- [41] Chenxin Tao, Xizhou Zhu, Gao Huang, Yu Qiao, Xiaogang Wang, and Jifeng Dai. Siamese image modeling for self-supervised vision representation learning. *arXiv preprint arXiv:2206.01204*, 2022. 6, 7
- [42] Zhan Tong, Yibing Song, Jue Wang, and Limin Wang. Video-MAE: Masked autoencoders are data-efficient learners for self-supervised video pre-training. In *Advances in Neural Information Processing Systems*, 2022. 7, 11
- [43] Hugo Touvron, Matthieu Cord, Matthijs Douze, Francisco Massa, Alexandre Sablayrolles, and Herve Jegou. Training data-efficient image transformers & distillation through attention. In *International Conference on Machine Learning*, volume 139, pages 10347–10357, July 2021. 2, 7
- [44] Liwei Wang, Chen-Yu Lee, Zhuowen Tu, and Svetlana Lazebnik. Training deeper convolutional networks with deep supervision. *arXiv preprint arXiv:1505.02496*, 2015. 3
- [45] Limin Wang, Zhan Tong, Bin Ji, and Gangshan Wu. TDN: Temporal difference networks for efficient action recognition. In *CVPR*, 2021. 7
- [46] Xiaolong Wang, Ross Girshick, Abhinav Gupta, and Kaiming He. Non-local neural networks. In *CVPR*, 2018. 7
- [47] Xinlong Wang, Rufeng Zhang, Chunhua Shen, Tao Kong, and Lei Li. Dense contrastive learning for self-supervised visual pre-training. In *Proceedings of the IEEE/CVF Conference on Computer Vision and Pattern Recognition*, pages 3024–3033, 2021. 3
- [48] Chen Wei, Haoqi Fan, Saining Xie, Chao-Yuan Wu, Alan Yuille, and Christoph Feichtenhofer. Masked feature prediction for self-supervised visual pre-training. In *CVPR*, pages 14668–14678. IEEE, 2022. 1, 2, 3, 4, 6, 8
- [49] Zhirong Wu, Yuanjun Xiong, Stella X Yu, and Dahua Lin. Unsupervised feature learning via non-parametric instance discrimination. In *Proceedings of the IEEE conference on computer vision and pattern recognition*, pages 3733–3742, 2018. 3
- [50] Tete Xiao, Yingcheng Liu, Bolei Zhou, Yuning Jiang, and Jian Sun. Unified perceptual parsing for scene understanding. In *ECCV*, pages 418–434. Springer, 2018. 6, 7, 11
- [51] Saining Xie and Zhuowen Tu. Holistically-nested edge detection. In *Proceedings of the IEEE international conference on computer vision*, pages 1395–1403, 2015. 1
- [52] Zhenda Xie, Zigang Geng, Jingcheng Hu, Zheng Zhang, Han Hu, and Yue Cao. Revealing the dark secrets of masked image modeling. *arXiv preprint arXiv:2205.13543*, 2022. 5
- [53] Zhenda Xie, Yutong Lin, Zheng Zhang, Yue Cao, Stephen Lin, and Han Hu. Propagate yourself: Exploring pixel-level consistency for unsupervised visual representation learning. In *Proceedings of the IEEE/CVF Conference on Computer Vision and Pattern Recognition*, pages 16684–16693, 2021. 3
- [54] Zhenda Xie, Zheng Zhang, Yue Cao, Yutong Lin, Jianmin Bao, Zhuliang Yao, Qi Dai, and Han Hu. Simmim: A simple framework for masked image modeling. In *CVPR*, pages 9653–9663. IEEE, 2022. 2, 3, 4, 6, 8
- [55] Zhenda Xie, Zheng Zhang, Yue Cao, Yutong Lin, Yixuan Wei, Qi Dai, and Han Hu. On data scaling in masked image modeling. *arXiv preprint arXiv:2206.04664*, 2022. 2, 4
- [56] Linfeng Zhang, Xin Chen, Junbo Zhang, Runpei Dong, and Kaisheng Ma. Contrastive deep supervision. In *Computer Vision—ECCV 2022: 17th European Conference, Tel Aviv, Israel, October 23–27, 2022, Proceedings, Part XXVI*, pages 1–19. Springer, 2022. 3
- [57] Bolei Zhou, Hang Zhao, Xavier Puig, Tete Xiao, Sanja Fidler, Adela Barriuso, and Antonio Torralba. Semantic understanding of scenes through the ade20k dataset. *IJCV*, 127(3):302–321, 2019. 6, 7, 11
- [58] Jinghao Zhou, Chen Wei, Huiyu Wang, Wei Shen, Cihang Xie, Alan Yuille, and Tao Kong. ibot: Image bert pre-training with online tokenizer. *ICLR*, 2022. 3, 6, 7

In this supplementary material, we first provide further implementation details (Appendix A). We then describe additional ablation studies (Appendix B).

A. More Implementation Details

Pretraining. We follow the same training recipe of MAE [15] and use a batch size of 4096 and a learning rate of $lr = base_lr \times BatchSize/256$, where $base_lr = 1.5e-4$. We adopt a cosine decay schedule with a warm-up for 40 epochs. We use AdamW [33] with a weight decay of 0.05 as the optimizer. For data augmentations, we use random resized cropping and random horizontal flipping. The mask ratio is set to 75% by default.

Finetuning on ImageNet-1K. ImageNet-1K [9] contains 1.28M images for training and 50K images for validation. We follow the same recipe of MAE [15] on ImageNet-1K except for the learning rate and layer decay. We adopt AdamW as the optimizer and finetune the pre-trained model for 100 epochs. The learning rate is set to $2e-4$ for DeepMIM on MAE-Pixel [15]/HOG [8]/DINO [4]/Codebook [11] and $4e-4$ for DeepMIM on MAE-CLIP. We adopt a cosine decay schedule with a warm-up for 5 epochs. The layer-wise learning rate decay is set to 0.65 for 300-epoch pre-trained model and 0.6 for 800-epoch pre-trained model. The batch size is set to 1024. For data augmentation and regularization, we adopt drop path with a drop path rate of 0.1, RandAugment, label smoothing of 0.1, Mixup of 0.8, CutMix of 1.0.

Finetuning on COCO Object Detection and Instance Segmentation. COCO [30] contains 118K images for training and 5K images for validation. Following [15], we adopt DeepMIM pre-trained ViT as the backbone and MaskRCNN [17] as the framework. For all DeepMIM pre-trained models, we use AdamW as the optimizer with a weight decay of 0.1. The learning rate, the layer-wise learning rate decay and the batch size is set to $1e-4$, 0.75 and 16, respectively. The input resolution is 1024×1024 . We do not use multi-scale testing.

Finetuning on ADK20K Semantic Segmentation. ADE20K [57] is a widely used dataset for semantic segmentation with 150 classes and 20K images for training and 2K images for validation. We use DeepMIM pre-trained ViT as the backbone and UperNet [50] as the segmentation model. We use AdamW as the optimizer with a weight decay of 0.05. We set drop path rate to 0.1, batch size to 16. For DeepMIM on MAE, the learning rate is set to $1e-4$, the layer-wise learning rate decay is set to 0.65. For DeepMIM on MAE-CLIP, the learning rate is set to $5e-5$, the layer-wise learning rate decay is set to 0.9. The input resolution is 512×512 . We do not use multi-scale testing.

Pre-training and Finetuning on Kinetics-400 Video Classification. DeepMIM on VideoMAE [42] is pre-trained for 800 epochs and finetuned for 75 epochs on Kinetics-400 video classification dataset. The optimizer, data augmenta-

Method	Masking Strategy	Top-1 Acc.
MAE	Random [15]	82.6
DeepMIM	Random [15]	83.6 (+1.0)
MAE	Semantic-guided [28]	82.8
DeepMIM	Semantic-guided [28]	83.8 (+1.0)
MAE	Semantic-aware [23]	82.9
DeepMIM	Semantic-aware [23]	83.8 (+0.9)

Table 12: DeepMIM is compatible with different masking strategies. The results are evaluated on ImageNet-1K finetuning.

tion and hyper-parameters are the same as when pre-training on ImageNet. We use a batch size of 1024 during pre-training. During finetuning, we use AdamW with a weight decay of 0.05 as the optimizer. The learning rate is set to $1e-3$. We adopt a cosine decay schedule with a warm-up for 5 epochs. The layer-wise learning rate decay is set to 0.75. For data augmentation and regularization, we adopt drop path with a drop path rate of 0.1, RandAugment, label smoothing of 0.1, Mixup of 0.8, CutMix of 1.0. We follow SlowFast [14] and take 5 clips \times 3 crops for inference.

B. More Ablation Studies

DeepMIM is Compatible with Different Masking Strategies. DeepMIM is compatible not only with different reconstruction targets at output level, but also with different masking strategies at input level. As shown in Table 12, DeepMIM consistently improves various MIM models with different masking strategies including random masking [15], semantic-guided masking [28] and semantic-aware masking [23].